Determination of bilayer membrane bending stiffness by tether formation from giant, thin-walled vesicles

Lin Bo and Richard E. Waugh
Department of Biophysics, University of Rochester, School of Medicine and Dentistry, Rochester, New York 14642

ABSTRACT The curvature elastic modulus (bending stiffness) of stearoyl-oleoyl phosphatidylcholine (SOPC) bilayer membrane is determined from membrane tether formation experiments. R. E. Waugh and R. M. Hochmuth 1987. *Biophys. J.* 52:391–400) have shown that the radius of a bilayer cylinder (tether) is inversely related to the force supported along its axis. The coefficient that relates the axial force on the tether to the tether radius is the membrane bending stiffness. Thus, the bending stiffness can be calculated directly from measurements of the tether radius as a function of force.

Giant (10–50-μm diam) thin-walled vesicles were aspirated into a micropipette and a tether was pulled out of the surface by gravitational forces on small glass beads that had adhered to the vesicle surface. Because the vesicle keeps constant surface area and volume, formation of the tether requires displacement of material from the projection of the vesicle in the pipette. Tethers can be made to grow longer or shorter or to maintain equilibrium by adjusting the aspiration pressure in the micropipette at constant tether force. The ratio of the change in the length of the tether to the change in the projection length is proportional to the ratio of the pipette radius to the tether radius. Thus, knowing the density and diameter of the glass beads and measuring the displacement of the projection as a function of tether length, independent determinations of the force on the tether and the tether radius were obtained. The bending stiffness for an SOPC bilayer obtained from these data is $\sim 2.0 \times 10^{-12}$ dyn cm, for tether radii in the range of 20–100 nm. An equilibrium relationship between pressure and tether force is derived which closely matches experimental observation.

INTRODUCTION

The phospholipid bilayer is a major constituent of virtually all biological membranes. Many biological processes require changes in the geometry of the cell surface and so can be affected by the intrinsic deformability of the membrane. Thus, the bending stiffness of the membrane plays a role in processes involving changes in membrane curvature, e.g., exocytosis (secretion), endocytosis, membrane fusion, cell division, and membrane remodeling during red cell maturation. Understanding the mechanical properties of bilayers and how they resist deformation will help us better understand such biological processes at a fundamental level.

Because biomembranes are very thin, the curvature elastic modulus is small, and it is difficult to measure experimentally. Several groups have estimated the curvature modulus by measuring the frequency of thermally driven fluctuations of the membrane contour. Servuss et al. (1976) and Schneider et al. (1984), using slightly different analytical approaches, each arrived at a value for the modulus in the range $1.0–2.5 \times 10^{-12}$ dyn cm (erg) for the curvature elastic modulus of egg lecithin bilayers. More recently, Duwe et al. (1987) obtained a value of 1.1×10^{-12} dyn cm for dimyristoyl phosphatidylcholine (DMPC) bilayers above the phase transition (26°C). (In a previous article from the same laboratory [Engelhardt et al., 1985] a smaller value was reported. The small value resulted from an error in calculation that was corrected in the later work.) The difference between these values may be attributable to differences in the bilayer composition (see Discussion), but it should also be recognized that the calculated value is sensitive to the different theoretical models used to obtain the modulus from experimental observations. This might account for disagreement among values of the bending modulus reported for the erythrocyte membrane. Brochard and Lennon (1975) analyzed the "flicker" of the red blood cell surface and estimated a value of $\sim 3.0 \times 10^{-13}$ dyn cm for that membrane. Using a distinctly different approach, Evans (1983) has estimated the bending stiffness of the red blood cell membrane from micropipet aspiration experiments. He finds a value of $\sim 1.8 \times 10^{-12}$ dyn cm.

In the present report we describe a new approach for measuring the bending stiffness of biological membranes at high curvatures. The technique involves the formation of cylindrical membrane strands (tethers) from large vesicular membranes. Recent theoretical work by Waugh

Address correspondence and reprint requests to Richard E. Waugh at the above address.

0006-3495/89/03/509/09 $2.00

and Hochmuth (1987) indicates that the membrane bending stiffness B relates the axial force on the tether f_t to its equilibrium radius R_t:

$$f_t = \frac{2\pi B}{R_t}. \quad (1)$$

(This result is not unique to the thick liquid shell model used by Waugh and Hochmuth, 1987. An identical relationship can be obtained using an energy-variational analysis of a thin cylindrical membrane with negligible surface shear rigidity, constant surface area, and finite curvature elasticity.) Thus, measurements of the force on the tether and the tether radius allow direct calculation of the membrane bending stiffness via Eq 1.

Tethers were first observed to be formed from red blood cells attached to a glass surface and subjected to fluid shear forces (Hochmuth et al., 1973). The tethers themselves were essentially invisible and the tether radii were unknown in those studies because the tether diameter (~100 nm) is too small to be resolved optically. Subsequently, Hochmuth et al. (1982) developed a new method for forming tethers from vesicular membranes (or erythrocytes) held in micropipets. Recognizing that the surface area and volume of the cell are conserved, they were able to calculate the radius of the tether by measuring the decrease in the length of the projection of the cell in the pipet for a given increase in the tether length (see Materials and Methods). Unfortunately, the force on the tether in those studies could not be measured, and had to be calculated based on assumptions about the equilibrium relationship between the tether force and the membrane force resultants on the body of the cell. (The present results indicate that these calculations were in error by approximately a factor of 2.0; see Discussion.) In the experiments described here tethers are formed by the negative buoyancy force of glass beads attached to the surface of phospholipid vesicles held in a micropipet. The density and diameter of the bead can be measured, and the radius of the tether can be determined by the method of Hochmuth and Evans (1982). The simultaneous and independent determinations of tether force and tether radius allow the direct calculation of the membrane bending stiffness via Eq. 1. Our results confirm that there is an inverse relation between tether radius and the force acting on the tether and indicate a value for the bending stiffness of SOPC bilayers of $\sim 2.0 \times 10^{-12}$ dyn cm.

MATERIALS AND METHODS

Preparation of vesicles

Vesicles were made by the modified method of Reeves and Dowben (1969) courtesy of David Needham (Duke University). SOPC (stearoyl-oleoyl-phosphatidylcholine) was dissolved in chloroform-methanol (2:1) at a concentration of 10 mg/ml. 30 μl of the SOPC solution was spread on a Teflon disk at the bottom of a 50-ml beaker. The beaker was placed in a desicator and evacuated for 2–3 h to remove solvent. The beaker was exposed to a gentle stream of water-saturated nitrogen for 20–30 min. Then, 8 ml of 100 mM sucrose solution was added and the lipid was left to stand overnight undisturbed at room temperature. The vesicles appeared as a white cloud near the Teflon surface. This suspension could be stored in a refrigerator for up to 1 wk.

At the time of the experiment, a small quantity of this suspension was dispersed into a glucose solution (100 mM) to make a working suspension. (The difference in refractive index between the glucose and sucrose solutions facilitated visualization of the vesicles by modulation contrast optics.)

Preparation of pipets

Pipets were made using a vertical pipet puller and a microforge. Needles with long tips were made from capillary tubing with a pipet puller. Then, the tips were broken off using the microforge to form pipets with inside diameters between 8.0 and 12.0 μm. Pipets were stored in small test tubes filled with filtered (0.2-μm pore size) glucose solution (100 mM). The tips of the pipets filled by capillary action. Before use, the remainder of the pipet was filled with glucose solution from the back with a 31-gauge needle.

Microchamber and microscope

The microchamber in which the experiments were performed was constructed of a plastic plate with a U-shaped cutout, a Teflon gasket, and two glass coverslips (Fig. 1). The chamber was mounted on a horizontal microscope (modified; Carl Zeiss Inc., Thornwood, NY), connected to two fluid reservoirs and filled with glucose solution (100 mM). The reservoir heights could be adjusted so that the velocity and direction of flow in the chamber could be controlled. (Experiments were performed with the fluid velocity set to zero.) The micropipet was mounted in a micromanipulator mounted above the chamber and the tip of the pipet was inserted into the open side of the "U." The microscope image was passed through a beam-splitter to two television cameras, one which provided a high magnification image for observing the length of the vesicle projecton in the pipet, and one that provided a low magnification image for observing the length of the tether. The images of the two cameras were mixed into a single split-screen image that could be displayed on a monitor and recorded on video tape for subsequent analysis. The pressure in the micropipet was controlled by adjusting the height of a water-filled reservoir connected to the back of the pipet. Zero pressure was determined by observing the flow of small particles at the tip of the pipet. Changes in pressure relative to zero were monitored with a pressure transducer (DP103; Validyne Engineering Corp., Northridge, CA) and the output of the transducer was incorporated into the recorded video picture.

Calibration of bead density

Glass beads with diameters between 10 and 30 μm were obtained from Polysciences, Inc. (Warrington, PA). The beads were found to adhere to the vesicles spontaneously, and no additional treatment of the beads was required. The density of the beads was determined from their settling velocity. Individual beads were picked up with a micropipet and dropped down the center of the rectangular channel. The drop was recorded on video tape, and the velocity of the bead and its diameter were measured from the recordings. The results are shown in Fig. 2. The solid curve is a single parameter least squares regression to the data assuming the

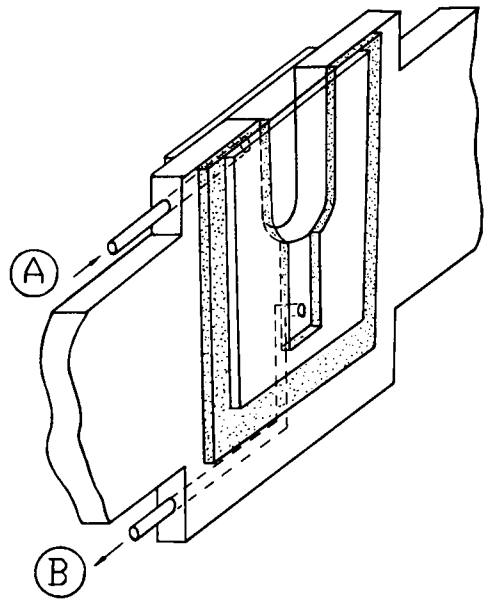

FIGURE 1 Schematic of the chamber used in the experiments. The chamber consisted of four layers in a sandwich—from left to right: Coverglass, plastic "frame," Teflon gasket, coverglass. A "U"-shaped cutout in the plastic frame served as a reservoir for vesicles and fluid and allowed introduction of the pipet from above. Port *A* was connected to a larger reservoir to maintain a constant fluid level in the chamber. The gasket was cut out to form a rectangular channel beneath the "U" between the frame and the coverglass. Vesicle–bead pairs were manipulated into the rectangular channel where the experiments were performed. Port *B* was connected through the plastic frame to the end of the rectangular channel and to a separate reservoir on a micrometer-positioned platform. The height of reservoir *B* could be adjusted to control the rate of flow in the channel.

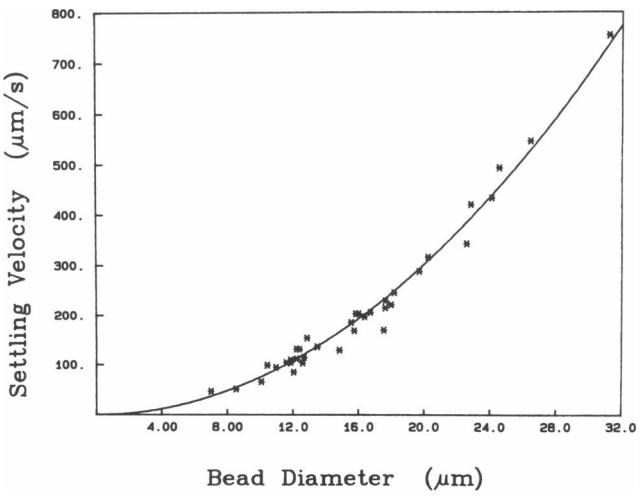

FIGURE 2 Settling velocity as a function of diameter for glass beads. Stars represent measurements on individual beads. The solid line is a one-parameter least-squares regression to the data according to Eq. 2. The value for the bead density from the regression is 2.39 g/cm^3.

following relationship between settling velocity, v, and bead diameter, D_b:

$$v = \frac{2}{9}\frac{g(\rho_B - \rho_f)}{\mu} D_b^2, \tag{2}$$

where ρ_B and ρ_f are the densities of the bead and fluid, respectively, μ is the viscosity of the fluid, and g is the acceleration of gravity. All of the parameters are known except the bead density, which is determined from the measurements. For individual measurements on 37 beads we obtained an average density of 2.38 g/cm^3 with a standard deviation of 0.16 g/cm^3. The value obtained by least-squares regression to all of the data was 2.39 g/cm^3. Using this value for the bead density, the force on the tether (at equilibrium in a still fluid) was calculated according to

$$f_b = \frac{4}{3}\pi R_b^3 g(\rho_B - \rho_f), \tag{3}$$

where R_b is the bead radius.

Procedure for measurement

Before introducing the vesicles, the chamber was filled with a solution containing 1 mg/ml BSA to reduce the charge on the glass surface. After rinsing, the chamber was filled with glucose solution and a few drops of the vesicle solution were introduced. Glass beads were put into the chamber and allowed to settle to the bottom of the "U." A vesicle was aspirated into the pipet, forming a spherical portion outside the pipet and a projection within the pipet (Fig. 3).

To form a tether the vesicle was placed in contact with a glass bead and allowed to stick to it, thus forming a vesicle–bead pair. The vesicle–bead pair was positioned in the rectangular channel at a measured distance from the glass slide and at a predetermined depth (~1.5 mm below the entrance to the channel) midway between the sides of the channel formed by the gasket. The aspiration pressure in the pipet was reduced until the bead fell away from the vesicle, forming a tether between the bead and the body of the vesicle. Then the pressure was increased and adjusted to stop the bead movement and establish equilibrium. Reducing the magnitude of the aspiration pressure caused the bead to move away from the vesicle drawing more material into the tether. Increasing the aspiration pressure caused the bead to move toward the vesicle as material was drawn from the tether back onto the body of the vesicle. The exchange of material between the vesicle and the tether was evidenced by the change in the length of the vesicle projection into the pipet. As the tether grew, the length of the projection decreased, and vice versa.

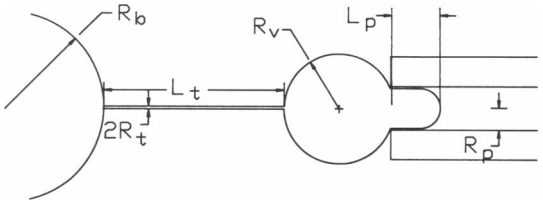

FIGURE 3 Schematic of tether formation. The vesicle was held in a micropipet (*right*) and tethered to a glass bead (*left*). The dimensions are labeled in the figure: pipet radius, R_p; projection length, L_p; vesicle radius, R_v; tether length, L_t; tether radius, R_t; and bead radius, R_b.

Calculations of tether radius

Hochmuth and Evans (1982) have introduced a relationship between tether radius, R_t, and the ratio of the change in projection length, L_p, to the corresponding change in tether length L_t:

$$R_t = \left(1 - \frac{R_p}{R_v}\right) R_p \left(-\frac{dL_p}{dL_t}\right), \quad (4)$$

where R_p is the pipet radius and R_v is the vesicle radius. All of the parameters on the right side of Eq. 4 are measurable, so the tether radius can be calculated from the data. The radius calculated via Eq. 4 represents a "mean-mass" radius of the tether. It is approximately equal to the radius of the mid-surface of the membrane.

Compressibility measurements

Compressibility measurements were performed on some vesicles before attachment to glass beads. The vesicle was aspirated into a micropipet and the projection was measured as a function of the pipet pressure. Thus, a series of data pairs of P_p and L_p were generated.

The isotropic membrane force resultant can be calculated from the applied pressure (Evans et al., 1976):

$$\bar{T} = \frac{\Delta P R_p}{2}\left(1 - \frac{R_p}{R_v}\right)^{-1}, \quad (5)$$

where ΔP is the difference between ambient pressure and the pressure within the pipet. The corresponding fractional change in vesicle area ($\alpha = \Delta A/A_o$) was calculated from the change in the length of the projection, $\Delta L = L_p - L_o$. The unstressed area, A_o, is given by

$$A_o = 4\pi R_v^2 + 2\pi L_p R_p - \pi R_p^2. \quad (6)$$

The change in area for a given change in projection length was calculated assuming that the vesicle volume was constant:

$$\Delta A = \pi[2R_p\Delta L_p + (8R_v^3 - 6\Delta L_p R_p^2)^{2/3} - 4R_v^2]. \quad (7)$$

(The assumption of constant volume is valid cause of the low permeability of the bilayer membrane to water [Evans and Needham, 1987].)

The expansivity modulus of the membrane K relates the isotropic force resultant to the fractional change in membrane area α (Evans et al., 1976):

$$\bar{T} = K\alpha. \quad (8)$$

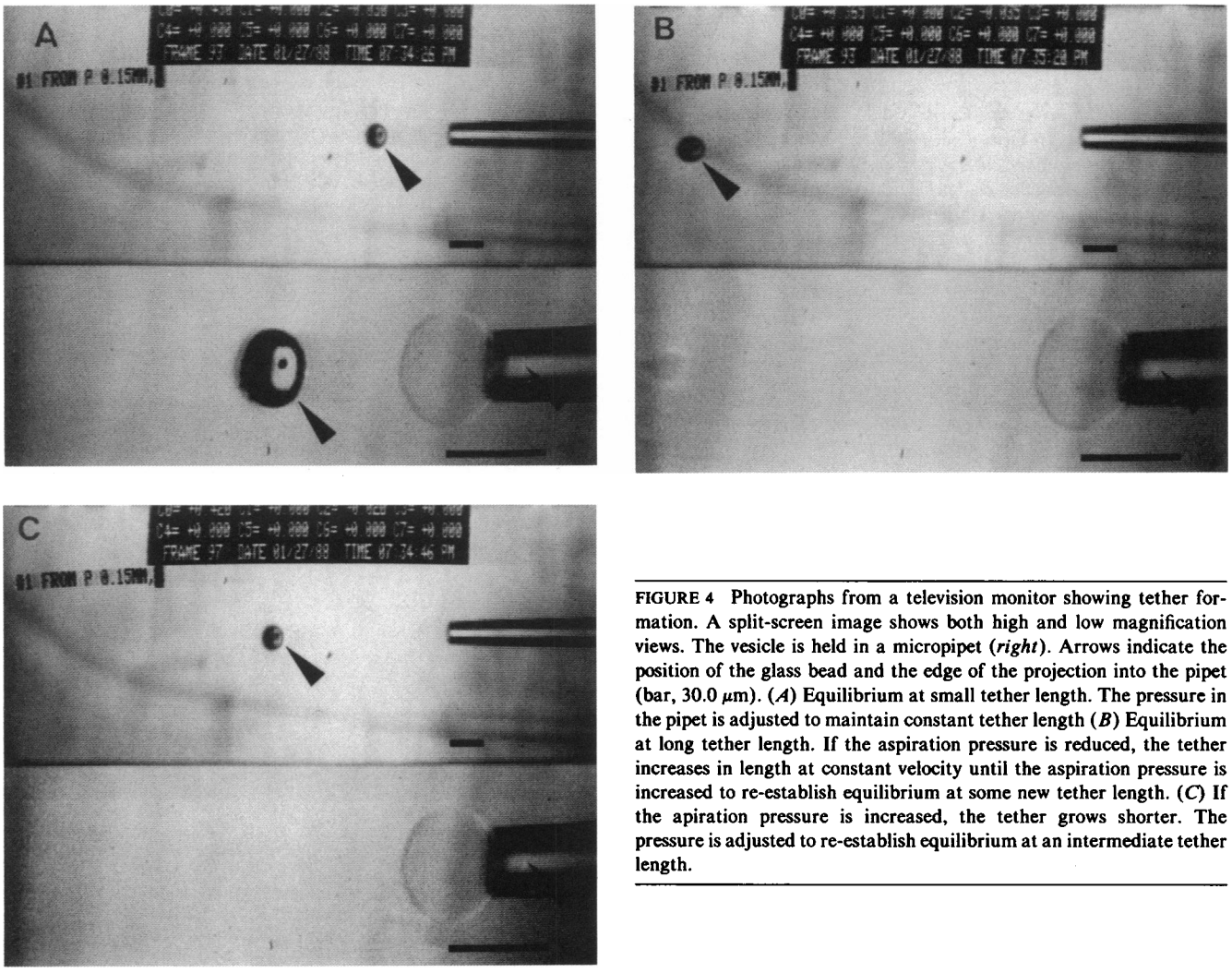

FIGURE 4 Photographs from a television monitor showing tether formation. A split-screen image shows both high and low magnification views. The vesicle is held in a micropipet (*right*). Arrows indicate the position of the glass bead and the edge of the projection into the pipet (bar, 30.0 μm). (*A*) Equilibrium at small tether length. The pressure in the pipet is adjusted to maintain constant tether length (*B*) Equilibrium at long tether length. If the aspiration pressure is reduced, the tether increases in length at constant velocity until the aspiration pressure is increased to re-establish equilibrium at some new tether length. (*C*) If the apiration pressure is increased, the tether grows shorter. The pressure is adjusted to re-establish equilibrium at an intermediate tether length.

The modulus was calculated by linear regression to the data. Care was taken that the projection lengths before and after the measurement were the same, to ensure that no additional area was incorporated into the surface (by fusion of small vesicles to the large vesicle) during the measurement.

RESULTS

Measurements were performed on a total of 24 tethers. Fig. 4 shows the process of tether formation. When the pipet suction was decreased, the bead began to separate from the vesicle (Fig. 4 *a*) and the tether formed between the body of the vesicle and the bead. Fig. 4 *b* and *c* shows the bead at equilibrium for different tether lengths. Occasionally, when the tether radius was large enough, a shadow of the tether could be seen on the monitor, but, in general, it was not visible because the radius was too small.

The tether length could be increased or decreased under constant force simply by adjusting the aspiration pressure in the pipet. Typically, once the vesicle–bead pair was formed, several "pulls" and "recoveries" were performed. The relationship between the projection length, L_p, and the tether length, L_t, was linear. Fig. 5 shows measurements of L_p as a function of L_t for three successive pulls and recoveries for a single vesicle–bead pair. Although all of the data fall in a narrow range, uncertainty in the determination of the slope, dL_p/dL_t, accounted for much of the scatter in our calculated values for R_t. For the three data sets shown in Fig. 5, the calculated tether radii ranged from 16.5 to 28.5 nm. The uncertainty was primarily due to difficulty in measuring the length of the projection in the pipet. Despite these measurement uncertainties, the calculated values for the membrane material properties fell in a narrow range (see Table 1). Over 80% of the values for B were between 1.0 and 3.0 $\times$ 10^{-12} dyn cm. The weighted mean for all the data was 2.0 $\times$ 10^{-12} dyn cm and the median was 1.9 $\times$ 10^{-12} dyn cm. The results of the present study are consistent with the theoretical expectations for an inverse relationship between tether force and tether radius (Eq. 1). The data are summarized in Fig. 6. Error bars indicate standard deviations for multiple measurements on the same tether at the same force. The solid curve was determined by least squares regression according to Eq. 1, with f_t as the independent variable. The value of B determined by the regression was 1.8 $\times$ 10^{-12} dyn cm.

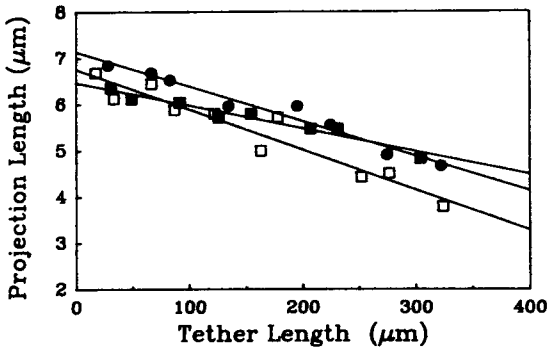

FIGURE 5 Length of the projection of the vesicle into the pipet as a function of the tether length. *Circles* and *open* and *solid squares* represent measurements for three successive pulls-and-recovery on the same tether. The data for the successive pulls fall in a narrow range. Solid lines are linear regressions to the three data sets. The tether radii determined from these data were 24.5, 28.5, and 16.5 nm.

Area expansivity measurements were performed on seven of the vesicles used in the tether experiments. The values for the moduli K are listed in Table 2 with the corresponding vesicle number. These values are consistent with other measurements of SOPC membrane area expansivity modulus performed in our laboratory as well as values reported in the literature (Evans and Needham, 1987). Although the values are scattered, there is no clear evidence that there were populations of vesicles with different lamellarity, and there was no correlation between the variability in bending stiffness and the corresponding value of K.

TABLE 1 Summary of tether formation data

Tether number	f	R_t	B	T	f_{th}/f_{meas}
	μdyn	*nm*	10^{-12} *dyn cm*	*dyn/cm*	
1	5.94	18.9	1.79	0.26	1.03
2	2.68	51.4	2.19	0.12	1.98
3	4.17	22.9	1.52	0.26	0.59
4	5.49	12.8	1.11	0.80	0.62
5	4.76	26.5	2.01	0.16	1.07
6	6.34	32.1	3.23	0.16	1.00
7	7.00	23.2	2.55	0.18	0.87
8	2.91	25.3	1.17	0.23	0.63
9	3.48	29.1	1.61	0.42	2.71
10	3.82	27.4	1.66	0.23	1.53
11	6.10	33.3	3.23	0.41	1.90
12	3.72	28.7	1.70	0.52	3.02
13	2.43	69.5	2.69	0.029	1.03
14	2.45	54.4	2.12	0.016	0.72
15	7.15	20.4	2.32	0.139	0.75
16	2.67	39.1	1.56	0.076	1.25
17	1.94	23.3	0.72	0.21	1.95
18*	2.11	53.1	1.79	0.049	1.27
19*	2.00	77.1	2.45	0.019	0.93
20*	1.15	81.7	1.50	0.015	1.13
21*	1.50	91.1	2.18	0.017	1.15
22	7.78	38.5	4.77	0.28	1.39
23	4.06	26.7	1.73	0.074	0.81
24	2.54	47.9	1.93	0.046	1.05

*Tethers 18 through 21 were pulled successively from the same vesicle using different glass beads.

TABLE 2 **Area expansivity modulus**

Vesicle number	B	K
	10^{-12} dyn cm	dyn/cm
1	1.79	179
2	2.19	341
5	2.01	314
6	3.23	156
9	1.61	113
10	1.66	537
11	3.23	170

DISCUSSION

Bending stiffness of phospholipid bilayer

Our results are in good agreement with determinations of the membrane bending stiffness of egg lecithin bilayers from thermal fluctuations. Servuss et al. (1976) obtained $B = 2.0–2.6 \times 10^{-12}$ ergs, and Schneider et al. (1984) obtained a value of $1.0–2.0 \times 10^{-12}$ ergs. Duwe et al. (1987) obtained a somewhat lower value for DMPC bilayers (1.1×10^{-12} ergs). The difference between Duwe's results and others are probably due to the different lipids used in the different studies. Waugh and Hochmuth (1987) and Evans and Skalak (1979) suggest that the bending stiffness of a membrane should depend on its expansivity modulus times the square of its thickness:

$$B \sim Kh^2. \tag{9}$$

The expansivity modulus for DMPC (in the liquid state) is reported to be 75% of the modulus for SOPC (Evans and Needham, 1987). Furthermore, DMPC has shorter hydrocarbon chains (14 versus 18 carbons) and so forms a thinner membrane. Thus, we expect DMPC membranes to have a bending modulus ~44% as large as that for SOPC membranes. With these considerations in mind, it appears that the data presently available are in excellent agreement.

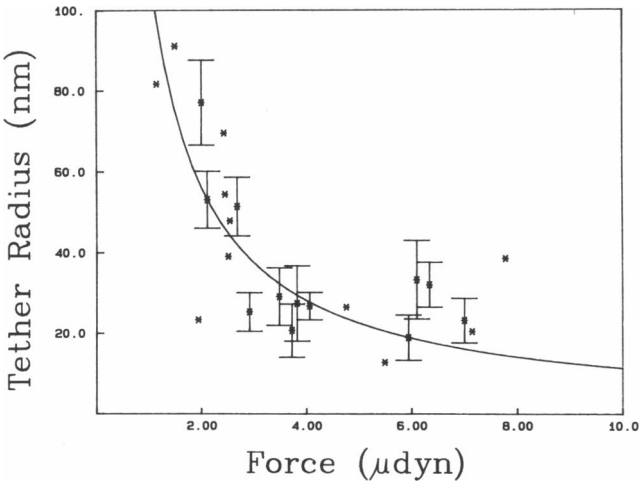

FIGURE 6 Tether radius as a function of the applied force. Stars represent mean values for extension and recovery of a single tether. Error bars represent standard deviations for multiple measurements on the same tether at the same force. The tether radii were calculated via Eq. 4 and the force was calculated according to Eq. 3. The solid line is a one-parameter least-squares regression to the data according to Eq. 1. The value of the membrane bending stiffness determined by the regression is 1.8×10^{-12} dyn cm.

Vesicle-tether equilibrium

Experimental observations show that a tether can be maintained at a constant length under an axial force by adjusting the aspiration pressure in the micropipet. This pressure is independent of the tether length. Understanding the conditions needed to establish equilibrium between the tether force and the pressure within the vesicle is important both for understanding the basic mechanics of tether formation as well as for establishing a basis for studying the resistance of cell membranes to loss of bilayer surface.

In previous mechanical analyses of membrane tether formation (Waugh, 1982; Hochmuth and Evans, 1982) the membrane was treated as a thin shell with negligible bending stiffness. This treatment together with the observation that phospholipid membranes have negligible surface shear rigidity leads to the prediction that the membrane force resultants are isotropic and constant over the surface of the vesicle. This in turn leads to a predicted relationship between the tether force, f_t, and the difference between the pressure inside the vesicle, P_v, and the pressure in the bathing fluid, P_o (Waugh, 1982):

$$f_t = \pi (P_v - P_o) R_v R_t. \tag{10}$$

Because this approach neglects membrane bending stiffness it fails to account for changes in the membrane force resultants in the vicinity of the tether that result from the membrane curvature elasticity. As a result, it leads to a major discontinuity in the membrane force resultants at the vesicle-tether junction (Waugh and Hochmuth, 1987). To remove this discontinuity, a more detailed mechanical analysis of the tether formation region (one which takes into account the finite thickness of the membrane) would be needed. Waugh and Hochmuth (1987) have solved this problem for the cylindrical tether, but direct solution of the equations of equilibrium for the internal membrane stresses on the vesicle surface in the vicinity of the tether is a formidable problem. Therefore,

to obtain an equilibrium relationship among the external forces on the vesicle we have resorted to an energy variational approach. This approach is detailed in the Appendix. It leads to the following result:

$$f_t \simeq \pi (P_v - P_o) R_v R_t + \frac{\pi B}{R_t}. \quad (11)$$

Note that the first term on the right-hand side of the equation is the thin membrane solution and the second term accounts for an additional force needed to bend the membrane into the high curvature of the tether. (The natural state of the membrane is assumed to be flat. A slightly different expression would be obtained if the membrane were allowed to have a natural or "spontaneous" curvature.) The experimental results are in good agreement with Eq. 11. Fig. 7 shows a histogram of the ratio of the theoretical versus the measured force. The median value is 1.06.

Bending stiffness of the red cell membrane

The revised equation for tether equilibrium (Eq. 11) can be used to re-evaluate the data on red cell tethers described by Waugh and Hochmuth (1987). Recall that only the tether radius and the aspiration pressure are known in those experiments, and that the force must be calculated from the pressure difference across the membrane. Previously, the equilibrium relationship for a thin membrane (Eq. 10) was used, and a value for B of 0.85×10^{-12} dyn cm was obtained from the red cell tether data. Using the revised equilibrium equation (Eq. 11) combined with the relationship between force and tether radius (Eq. 1) a new relationship between force and pressure is obtained:

$$f_t \simeq 2\pi (P_v - P_o) R_v R_t. \quad (12)$$

Thus, the thin membrane theory (Eq. 10) is in error by approximately a factor of 2.0. (Note that Eq. 12 presumes that the natural curvature of the membrane is zero, i.e., flat.) Applying this result (Eq. 12) to the red cell tether data results in a value for the bending stiffness that is larger than the original estimate by a factor of 2.0: $B = f_t R_t / 2\pi = 1.7 \times 10^{-12}$ dyn cm. This result is in excellent agreement with the value obtained by Evans (1983) from micropipet aspiration studies ($B = 1.8 \times 10^{-12}$ dyn cm). Waugh and Hochmuth (1987) also derived expressions relating the bending stiffness to the membrane area expansivity. Based on their underestimate of B, a value for the membrane expansivity modulus of 250 dyn/cm was calculated. Using the revised estimate of B based on Eq. 12, a value of 500 dyn/cm is obtained, which is in better agreement with the literature value of 450 dyn/cm (Evans and Waugh, 1977).

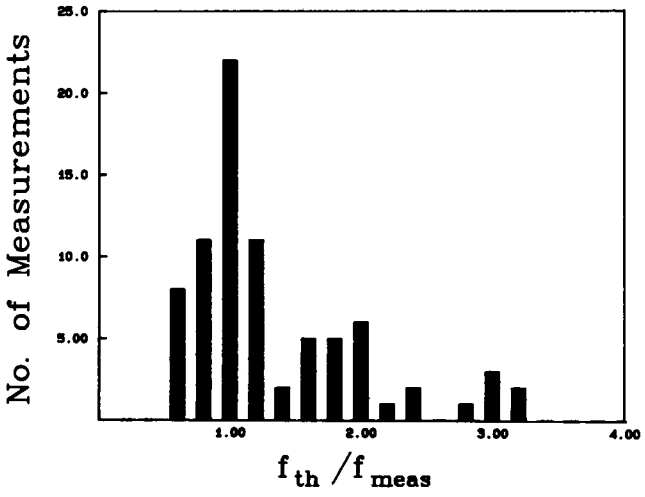

FIGURE 7 Histogram of the ratio of the theoretical force to the measured force. Separate determinations were made for each pull and each recovery. The theoretical force was calculated from Eq. 11. The value for R_v was measured directly and R_t was calculated via Eq. 4. P_v was calculated from the applied pressure difference, $P_p - P_o$, from force balance $P_v - P_o \simeq (P_p - P_o)/(R_v/R_p - 1.0)$. The value for B was determined independently for each measured value of f_t and corresponding value of R_t via Eq. 1. The measured force was obtained from Eq. 3. The median value for the ratio was 1.06.

CONCLUSIONS

A new approach for determining the bending stiffness of biological membranes is presented. The results yield a value for the membrane bending stiffness of SOPC bilayers of $\sim 2.0 \times 10^{-12}$ dyn cm. The results also verify a revised equation of equilibrium relating the tether force to the pipet aspiration pressure. Applying the revised equilibrium equation to measurements of tether formation from erythrocytes yields a value of 1.7×10^{-12} dyn cm for that membrane, in good agreement with the value previously determined by Evans (1983).

APPENDIX

Variational approach to vesicle-tether equilibrium

To obtain the relationship among the external forces on a tethered vesicle at equilibrium, we considered the variation in free energy for an arbitrary displacement of the tether length under a constant force (see Fig. A1). The system is approximated as a spherical vesicle (radius R_v), a cylindrical projection in the pipette with a hemispherical cap (radius

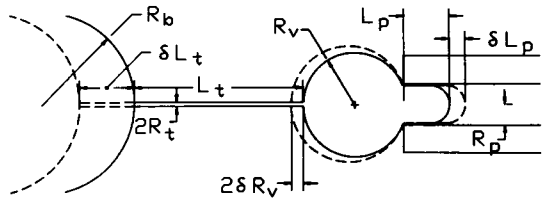

FIGURE A1 Illustrations of the virtual displacements of the vesicle dimensions for obtaining an equilibrium relationship between tether force and pressure by a variational approach. Variations in projection length, L_p, tether length, L_t, and vesicle radius, R_v, are illustrated by dashed lines. The displacements in the figure are shown in the positive sense.

R_p, length L_p) and a cylindrical tether (length L_t, radius R_t). The radius of the tether is functionally related to the force on the tether (Eq. 1) and so is assumed to remain constant during the variation. The vesicle radius, the length of the projection in the pipette, and the tether length are free to vary. The pipette is taken to be stationary. The major assumptions are: (*a*) the fluid within and surrounding the vesicle is incompressible; (*b*) the area of the membrane is fixed; (*c*) the membrane has zero surface shear rigidity; and (*d*) the membrane stores energy elastically when it bends. The change in free energy with bending is assumed to take the form (Evans and Skalak, 1979):

$$\Delta F/A_o = B\,(C_1 + C_2)^2/2, \tag{A1}$$

where C_1 and C_2 are the change in the principal curvatures relative to the unstressed state. Thus the change in free energy due to elastic deformation of the system for the virtual displacement is simply the energy required to bend the membrane as it moves from the vesicle surface into the tether. The total variation in free energy for a virtual displacement of the vesicle dimensions is

$$\delta F = (P_v - P_o)\,(\delta V_s + \pi R_t^2 \delta L_t) + (P_v - P_p)\,\delta V_p + f_t\,(\delta L_t + 2\delta R_v) - \frac{1}{2} B\,(\Delta C)^2\,\delta(2\pi R_t L_t), \tag{A2}$$

where V_s is the volume of the sphere, V_p is the volume within the pipette, and ΔC is the difference in the total membrane curvature between the vesicle body and the tether. Because $R_v \gg R_t$ we approximate ΔC as $1.0/R_t$. In terms of the vesicle dimensions, Eq. A2 can be written (for $L_p \geq R_p$):

$$\delta F = (P_v - P_o)\,(4\pi R_v^2 \delta R_v + \pi R_t^2\,\delta L_t) + (P_v - P_p)\,(\pi R_p^2 \delta L_p) + f_t\,(\delta L_t + 2\,\delta R_v) - \frac{\pi B}{R_t}\,\delta L_t. \tag{A3}$$

The variation is subject to the additional constraints that the total surface area and volume are constant:

$$\delta A \simeq 8\pi R_v \delta R_v + 2\pi R_t \delta L_t + 2\pi R_p \delta L_p = 0, \tag{A4}$$

and

$$\delta V \simeq 4\pi R_v^2 \delta R_v + \pi R_p^2 \delta L_p + \pi R_t^2 \delta L_t = 0. \tag{A5}$$

The approximation symbol indicates that the change in the overlap of the sphere (radius R_v) with the pipet cylinder has been neglected. Eqs. A3, A4, and A5 can be solved to eliminate δR_v and δL_p, and an expression in terms of δL_t is obtained:

$$\delta F = \left[\frac{\pi (P_p - P_o) R_v R_t}{\frac{R_v}{R_p} - 1.0} - \frac{\pi B}{R_t} + f_t\right] \delta L_t, \tag{A6}$$

where terms of order R_t/R_v have been neglected compared to 1.0. At equilibrium the variation in energy must be zero, and we obtain

$$f_t \simeq \frac{\pi (P_o - P_p) R_v R_t}{\frac{R_v}{R_p} - 1.0} + \frac{\pi B}{R_t}. \tag{A7}$$

The first term can be re-expressed (approximately) in terms of $P_v - P_o$, the transmembrane pressure difference:

$$f_t \simeq \pi\,(P_v - P_o)\,R_v R_t + \frac{\pi B}{R_t}. \tag{A8}$$

Note that the first term represents the thin membrane solution and the second term gives the additional contribution due to the bending stiffness of the membrane.

The authors thank Dr. David Needham for his protocol for making giant thin-walled vesicles. The authors also acknowledge Drs. S. Svetina and B. Zeks for their helpful discussions about the variational approach to obtain the equilibrium condition for tether force and pressure. The authors recognize the technical support of David Coleman, who made measurements of the glass bead density, and Richard Bauserman, who assisted with chamber design and manufacture and prepared photographic materials for publication.

This work was supported by the Public Health Service under National Institutes of Health grants HL31524 and HL18208.

Received for publication 12 July 1988 and in final form 17 November 1988.

REFERENCES

Brochard, F., and J. F. Lennon. 1975. Frequency spectrum of the flicker phenomenon in erythrocytes. *J. Phys. (Paris)*. 36:1035–1047.

Duwe, H. -P., H. E. Engelhardt, A. Zilker, and E. Sackmann. 1987. Curvature elasticity of smectic A lipid bilayers and cell plasma membranes. *Mol. Cryst. Liq. Crys.* 152:1–7.

Engelhardt, H., H. P. Duwe, and E. Sachman. 1985. Bilayer bending elasticity measured by Fourier analysis of thermally excited surface undulations of flaccid vesicles. *J. Phys. Lett.* 46:L395–L400.

Evans, E. A. 1983. Bending elastic modulus of red blood cell membrane derived from buckling instability in mircopipette aspiration tests. *Biophys. J.* 43:27–30.

Evans, E., and D. Needham. 1987. Physical properties of surfactant bilayer membranes: thermal transitions, elasticity, rigidity, cohesion, and colloidal interactions. *J. Phys. Chem.* 91:4219–4228.

Evans, E. A., and R. Skalak. 1979. Mechanics and thermodynamics of biomembranes. *CRC Crit. Rev. Bioeng.* 3:181–418.

Evans, E. A., and R. Waugh. 1977. Osmotic correction to elastic area

compressibility measurements on red cell membrane. *Biophys. J.* 20:307–313.

Evans, E. A., R. Waugh, and L. Melnik. 1976. Elastic area compressibility modulus of red cell membrane. *Biophys. J.* 16:585–595.

Hochmuth, R. M., and E. A. Evans. 1982. Extensional flow of erythrocyte membrane from cell body to elastic tether: I. Analysis. *Biophys. J.* 39:71–81.

Hochmuth, R. M., N. Mohandas, and P. L. Blackshear, Jr. 1973. Measurement of the elastic modulus for red cell membrane using a fluid mechanical technique. *Biophys. J.* 13:747–762.

Hochmuth, R. M., H. C. Wiles, E. A. Evans, and J. T. McCown. 1982. Extensional flow of erythrocyte membrane from cell body to elastic tether: II. Experiment. *Biophys. J.* 39:83–89.

Reeves, J. P., and R. M. Dowben. 1969. Formation and properties of thin-walled phospholipid vesicles. *J. Cell Physiol.* 73:49–60.

Schneider, M. B., J. T. Jenkins, and W. W. Webb. 1984. Thermal fluctuations of large cylindrical phospholipid vesicles. *Biophys. J.* 45:891–899.

Servuss, R. M., W. Harbich, and W. Helfrich. 1976. Measurement of the curvature-elastic modulus of egg lecithin bilayers. *Biochim. Biophys. Acta.* 436:900–903.

Waugh, R. E. 1982. Surface viscosity measurements from large bilayer vesicle tether formation: I. Analysis. *Biophys. J.* 38:19–27.

Waugh, R. E., and R. M. Hochmuth. 1987. Mechanical equilibrium of thick hollow liquid membrane cylinders. *Biophys. J.* 52:391–400.